

# Quartic inflation and radiative corrections with non-minimal coupling

**Nilay Bostan,**<sup>a,b</sup> **and Vedat Nefer Senoḡuz**<sup>a,\*</sup>

<sup>a</sup>Department of Physics, Mimar Sinan Fine Arts University,  
34380 Şişli, İstanbul, Turkey

<sup>b</sup>Department of Physics and Astronomy, University of Iowa,  
52242, Iowa, IA, USA

E-mail: [nilay-bostan@uiowa.edu](mailto:nilay-bostan@uiowa.edu), [nefer.senoguz@msgsu.edu.tr](mailto:nefer.senoguz@msgsu.edu.tr)

**Abstract.** It is well known that the non-minimal coupling  $\xi\phi^2R$  between the inflaton and the Ricci scalar affects predictions of single field inflation models. In particular, the  $\lambda\phi^4$  quartic inflation potential with  $\xi \gtrsim 0.005$  is one of the simplest models that agree with the current data. After reviewing the inflationary predictions of this potential, we analyze the effects of the radiative corrections due to couplings of the inflaton to other scalar fields or fermions. Using two different prescriptions discussed in the literature, we calculate the range of these coupling parameter values for which the spectral index  $n_s$  and the tensor-to-scalar ratio  $r$  are in agreement with the data taken by the Keck Array/BICEP2 and Planck collaborations.

**Keywords:** physics of the early universe, inflation

---

\*Corresponding author.

---

## Contents

|          |   |           |
|----------|---|-----------|
| <b>1</b> | <b>Introduction</b>   | <b>1</b>  |
| <b>2</b> | <b>Inflation with non-minimal coupling</b>                      | <b>2</b>  |
| <b>3</b> | <b>Quartic potential</b>  | <b>4</b>  |
| <b>4</b> | <b>Radiative corrections</b>                                    | <b>7</b>  |
| <b>5</b> | <b>Radiatively corrected quartic potential: Prescription I</b>  | <b>8</b>  |
| <b>6</b> | <b>Radiatively corrected quartic potential: Prescription II</b> | <b>12</b> |
| <b>7</b> | <b>Conclusion</b>   | <b>14</b> |

---

### 1 Introduction

Inflation [1–4], which is an accelerated expansion era thought to occur in the early universe, both helps explaining general properties of the universe such as its flatness and large scale homogeneity, and it leads to the primordial density perturbations that evolve into the structures in the universe. Up to now many inflationary models have been introduced with most of them depending on a scalar field called the inflaton. Predictions of these models are being tested by the cosmic microwave background radiation temperature anisotropies and polarization observations that have become even more sensitive in recent years [5, 6].

The observational parameter values predicted by different potentials that the inflaton may have were calculated in many articles, see for instance ref. [7]. A vast majority of these articles assume that the inflaton is coupled to gravitation solely through the metric. On the other hand the action in general also contains a coupling term  $\xi\phi^2R$  between the Ricci scalar and the inflaton (this is required by the renormalizability of the scalar field theory in curved space-time [8–10]), and inflationary predictions are significantly altered depending on the coefficient of this term [11–19].

In this work, we first review in section 2 how to calculate the main observables, namely the spectral index  $n_s$  and the tensor-to-scalar ratio  $r$ , for an inflaton potential in the presence of non-minimal coupling. Next, in section 3 we review the  $\lambda\phi^4$  quartic potential, providing analytical approximations for  $n_s$  and  $r$ , and showing that the model agrees with current data for  $\xi \gtrsim 0.005$ . We also briefly discuss how and to what extent can the reheating stage affect the values of observables.

Section 4 introduces two prescriptions that can be used to calculate radiative corrections to the inflaton potential due to inflaton couplings to bosons or fermions. In prescription I, a conformal transformation is applied to express the action in the Einstein frame; and the field dependent mass terms in the one-loop Coleman-Weinberg potential are expressed in this frame. Whereas in prescription II, the field dependent mass terms are taken into account in the original Jordan frame.

The next two sections, section 5 and section 6 contain a detailed numerical investigation of how the radiative corrections due to inflaton couplings to bosons or fermions modify the

predictions of the non-minimal quartic potential, for each prescription. We summarize our results in section 7.

The effect of radiative corrections to the predictions of the non-minimal quartic potential has been discussed mostly in the context of standard model (SM) Higgs inflation [20], see for instance ref. [21] and the references within. In this context, since the self coupling  $\lambda$  of the inflaton is known,  $\xi \gg 1$  is required [22]. In this limit, the observational parameters are given in terms of the e-fold number  $N$  by  $n_s \approx 1 - 2/N$  ve  $r \approx 12/N^2$  [23, 24] as in the Starobinsky model [25, 26]. Radiative corrections lead to deviations from this so called Starobinsky point in the  $n_s$  and  $r$  plane, however the size of these deviations differ according to the prescription used for the calculation. As discussed in refs. [21, 22, 27], the plateau type structure of the Einstein frame potential remains intact and the deviations in  $n_s$  are rather insignificant according to prescription I. However, according to prescription II, radiative corrections lead to a linear term in the Einstein frame potential written in terms of a scalar field with a canonical kinetic term. If the inflaton is dominantly coupling to bosons the coefficient of this term is positive, and as this coefficient is increased the inflationary predictions move towards the linear potential predictions  $n_s \approx 1 - 3/(2N)$  and  $r \approx 4/N$  [7]. If the inflaton is dominantly coupling to fermions the coefficient of this term is negative, leading to a reduction in the values of  $n_s$  and  $r$  [28].

In this work we take the inflaton to be a SM singlet scalar field, and take the self-coupling  $\lambda$  and  $\xi$  to be free parameters, with  $\xi \lesssim 10^3$  as discussed in section 3. Radiative corrections for a SM singlet inflaton have been studied by refs. [29–31]. Unlike these works, we focus on studying the effect of radiative corrections for general values of  $\xi \lesssim 10^3$ , including the case of  $\xi \ll 1$ . A related work which includes the case of  $\xi \ll 1$  is ref. [28]. In this work the inflaton is assumed to couple to fermions and prescription II is used. Ref. [32] considers a potential which coincides with the potential discussed in section 6 for inflaton coupling to bosons.<sup>1</sup> Here, we extend previous works by considering both prescriptions I and II, and inflaton coupling to bosons or fermions. For each case we calculate the regions in the plane of coupling parameter values for which the spectral index  $n_s$  and the tensor-to-scalar ratio  $r$  are in agreement with the current data. We also display how  $n_s$  and  $r$  change due to radiative corrections in these regions.

## 2 Inflation with non-minimal coupling

Consider a non-minimally coupled scalar field  $\phi$  with a canonical kinetic term and a potential  $V_J(\phi)$ :

$$\frac{\mathcal{L}_J}{\sqrt{-g}} = \frac{1}{2}F(\phi)R - \frac{1}{2}g^{\mu\nu}\partial_\mu\phi\partial_\nu\phi - V_J(\phi), \quad (2.1)$$

where the subscript  $J$  indicates that the Lagrangian is specified in Jordan frame, and  $F(\phi) = 1 + \xi\phi^2$ . We are using units where the reduced Planck scale  $m_P = 1/\sqrt{8\pi G} \approx 2.4 \times 10^{18}$  GeV is set equal to unity, so we require  $F(\phi) \rightarrow 1$  or  $\phi \rightarrow 0$  after inflation.

For calculating the observational parameters given eq. (2.1), it is convenient to switch to the Einstein ( $E$ ) frame by applying a Weyl rescaling  $g_{\mu\nu} = \tilde{g}_{\mu\nu}/F(\phi)$ , so that the Lagrangian density takes the form [37]

$$\frac{\mathcal{L}_E}{\sqrt{-\tilde{g}}} = \frac{1}{2}\tilde{R} - \frac{1}{2Z(\phi)}\tilde{g}^{\mu\nu}\partial_\mu\phi\partial_\nu\phi - V(\phi), \quad (2.2)$$

---

<sup>1</sup>See also refs. [33–36] for related work.

where

$$\frac{1}{Z(\phi)} = \frac{3}{2} \frac{F'(\phi)^2}{F(\phi)^2} + \frac{1}{F(\phi)}, \quad V(\phi) = \frac{V_J(\phi)}{F(\phi)^2}, \quad (2.3)$$

and  $F' \equiv dF/d\phi$ . If we make a field redefinition

$$d\sigma = \frac{d\phi}{\sqrt{Z(\phi)}}, \quad (2.4)$$

we obtain the Lagrangian density for a minimally coupled scalar field  $\sigma$  with a canonical kinetic term.

Once the Einstein frame potential is expressed in terms of the canonical  $\sigma$  field, the observational parameters can be calculated using the slow-roll parameters (see ref. [38] for a review and references):

$$\epsilon = \frac{1}{2} \left( \frac{V_\sigma}{V} \right)^2, \quad \eta = \frac{V_{\sigma\sigma}}{V}, \quad (2.5)$$

where  $\sigma$ 's in the subscript denote derivatives. The spectral index  $n_s$ , the tensor-to-scalar ratio and  $r$  are given in the slow-roll approximation by

$$n_s = 1 - 6\epsilon + 2\eta, \quad r = 16\epsilon. \quad (2.6)$$

The amplitude of the curvature perturbation  $\Delta_{\mathcal{R}}$  is given by

$$\Delta_{\mathcal{R}} = \frac{1}{2\sqrt{3}\pi} \frac{V^{3/2}}{|V_\sigma|}, \quad (2.7)$$

which should satisfy  $\Delta_{\mathcal{R}}^2 \approx 2.4 \times 10^{-9}$  from the Planck measurement [5] with the pivot scale chosen at  $k_* = 0.002 \text{ Mpc}^{-1}$ . The number of e-folds is given by

$$N_* = \int_{\sigma_e}^{\sigma_*} \frac{V d\sigma}{V_\sigma}, \quad (2.8)$$

where the subscript “ $*$ ” denotes quantities when the scale corresponding to  $k_*$  exited the horizon, and  $\sigma_e$  is the inflaton value at the end of inflation, which can be estimated by  $\epsilon(\sigma_e) = 1$ .

It is convenient for numerical calculations to rewrite these slow-roll expressions in terms of the original field  $\phi$ , following the approach in e.g. ref. [39]. Using eq. (2.4), eq. (2.5) can be written as

$$\epsilon = Z\epsilon_\phi, \quad \eta = Z\eta_\phi + \text{sgn}(V')Z' \sqrt{\frac{\epsilon_\phi}{2}}, \quad (2.9)$$

where we defined

$$\epsilon_\phi = \frac{1}{2} \left( \frac{V'}{V} \right)^2, \quad \eta_\phi = \frac{V''}{V}. \quad (2.10)$$

Similarly, eqs. (2.7) and (2.8) can be written as

$$\Delta_R = \frac{1}{2\sqrt{3}\pi} \frac{V^{3/2}}{\sqrt{Z}|V'|}, \quad (2.11)$$

$$N_* = \text{sgn}(V') \int_{\phi_e}^{\phi_*} \frac{d\phi}{Z(\phi)\sqrt{2\epsilon_\phi}}. \quad (2.12)$$

To calculate the numerical values of  $n_s$  and  $r$  we also need a numerical value of  $N_*$ . Assuming a standard thermal history after inflation,

$$N_* \approx 64.7 + \frac{1}{2} \ln \frac{\rho_*}{m_P^4} - \frac{1}{3(1+\omega_r)} \ln \frac{\rho_e}{m_P^4} + \left( \frac{1}{3(1+\omega_r)} - \frac{1}{4} \right) \ln \frac{\rho_r}{m_P^4}. \quad (2.13)$$

Here  $\rho_e = (3/2)V(\phi_e)$  is the energy density at the end of inflation,  $\rho_* \approx V(\phi_*)$  is the energy density when the scale corresponding to  $k_*$  exited the horizon,  $\rho_r$  is the energy density at the end of reheating and  $\omega_r$  is the equation of state parameter during reheating.<sup>2</sup> As discussed in section 3,  $\omega_r = 1/3$  is generally a good approximation for the potentials which we investigate. For this case

$$N_* \approx 64.7 + \frac{1}{2} \ln \rho_* - \frac{1}{4} \ln \rho_e, \quad (2.14)$$

independent of the reheat temperature.

### 3 Quartic potential

Inflationary predictions of non-minimal quartic inflation have been studied in detail, see e.g. refs. [14, 15, 24, 28, 41–43]. Here after summarizing the results following ref. [43], we comment on an analytical approximation used in that work, and briefly discuss the effect of the reheating stage on the inflationary predictions.

In Einstein frame, the non-minimal quartic inflation potential is

$$V(\phi) = \frac{(1/4)\lambda\phi^4}{(1+\xi\phi^2)^2}. \quad (3.1)$$

Using eqs. (2.6) and (2.9), we obtain

$$\begin{aligned} n_s &= 1 - \frac{24}{\phi^2} \left( \frac{1 + \frac{5}{3}\psi + 8\xi\psi + \frac{2}{3}\psi^2 + 4\xi\psi^2}{(1 + (1 + 6\xi)\psi)^2} \right), \\ r &= \frac{128}{\phi^2} \frac{1}{1 + (1 + 6\xi)\psi}, \end{aligned} \quad (3.2)$$

where we defined  $\psi \equiv \xi\phi^2$ . Using eq. (2.11) we obtain

$$\lambda = 12\pi^2 \Delta_R^2 \frac{64(1+\psi)^2 \xi^3}{\psi^2(1 + (1 + 6\xi)\psi)}, \quad (3.3)$$

and using eq. (2.12) we obtain

$$N = \frac{3}{4s}(\psi - \psi_e) - \frac{3}{4} \ln \frac{1+\psi}{1+\psi_e}, \quad (3.4)$$

---

<sup>2</sup>For a derivation of eq. (2.13) see e.g. ref. [40].

where  $s \equiv (6\xi)/(1 + 6\xi)$ . Here  $\psi_e$  can be obtained from  $\epsilon(\psi_e) = 1$  as follows:

$$\psi_e = \frac{-1 + \sqrt{1 + 32\xi(1 + 6\xi)}}{2(1 + 6\xi)}. \quad (3.5)$$

For any value of  $\xi$ , we can calculate the observational parameters by numerically solving eqs. (3.4) and (2.14) (with a correction for  $\xi \gtrsim 1$ , see below for a discussion) to find the value of  $\phi_*$ . Formally, inverting eq. (3.4) gives a solution in terms of the  $-1$  branch of the Lambert function:

$$\psi = -sW_{-1}\left(-\frac{e^{-1/s}}{s \exp[4N/3 + \psi_e/s - \ln(1 + \psi_e)]}\right) - 1. \quad (3.6)$$

As ref. [43] point out, one can find reasonable approximations to the numerical solution by utilizing  $N + 1 \approx 3\psi/(4s)$ . Here we point out that a slightly more complicated but better approximation can be obtained by using  $W_{-1}(-x) \approx \ln x - \ln(-\ln x)$ :

$$\psi \approx \frac{4sN}{3} + s \ln\left(1 + \frac{4sN}{3}\right). \quad (3.7)$$

Inserting eq. (3.7) in eqs. (3.2) and (3.3), we obtain the eqs. (3.19), (3.20) and (3.22) in ref. [43] only with the modification

$$N + 1 \rightarrow N' \equiv N \left[ 1 + \frac{3}{4N} \ln\left(1 + \frac{4sN}{3}\right) \right]. \quad (3.8)$$

Comparison of the numerical solutions and the two analytical approximations discussed here is shown in figure 1. As can be seen from the figure, our analytical approximation is more accurate for  $\xi \gg 1$ , and  $n_s$  ( $r$ ) values deviate from the numerical solution by at most 2% (3%) for any  $\xi$  value.

For the minimally coupled case, quartic potential implies an equation of state parameter  $\omega_r = 1/3$  after inflation [45], and as a result the number of e-folds  $N_*$  is given by eq. (2.14), independent of the reheat temperature. This result, which removes the uncertainty in the observational parameter values due to the reheat temperature, is also valid for  $\xi \lesssim 1$ . However, for  $\xi \gtrsim 1$  the reheating stage includes a phase where the Einstein frame potential for the canonical scalar field is quadratic. Following refs. [46, 47], we obtain the e-fold number in this case as

$$N_* \approx 64.7 + \frac{1}{2} \ln \frac{\rho_*}{m_P^4} - \frac{1}{3} \ln \frac{\rho_e}{m_P^4} + \frac{1}{12} \ln \frac{V(\phi = \sqrt{2}/(3^{1/4}\xi))}{m_P^4}. \quad (3.9)$$

For  $\xi \gtrsim 1$  we use this expression instead of eq. (2.14) in figure 1. The quadratic phase slightly reduces the value of  $N_*$  with respect to the value calculated by eq. (2.14). The difference in  $N_*$  between the two expressions is approximately given by

$$\frac{1}{12} \ln \frac{V\left(\phi = \frac{\sqrt{2}}{3^{1/4}\xi}\right)}{\rho_e}. \quad (3.10)$$

Since  $\xi\phi^2 \lesssim 1$ ,  $V(\phi) \propto \phi^4$  after inflation. In this case  $\rho_e$  is proportional to  $\phi_e^4 = 4/(3\xi^2)$  for  $\xi \gg 1$ . Thus, for  $\xi \gg 1$ , the reduction in  $N_*$  due to the quadratic phase is approximately given by  $-(1/6) \ln \xi$  [47].

For the non-minimal quartic potential, expanding the action around the vacuum reveals

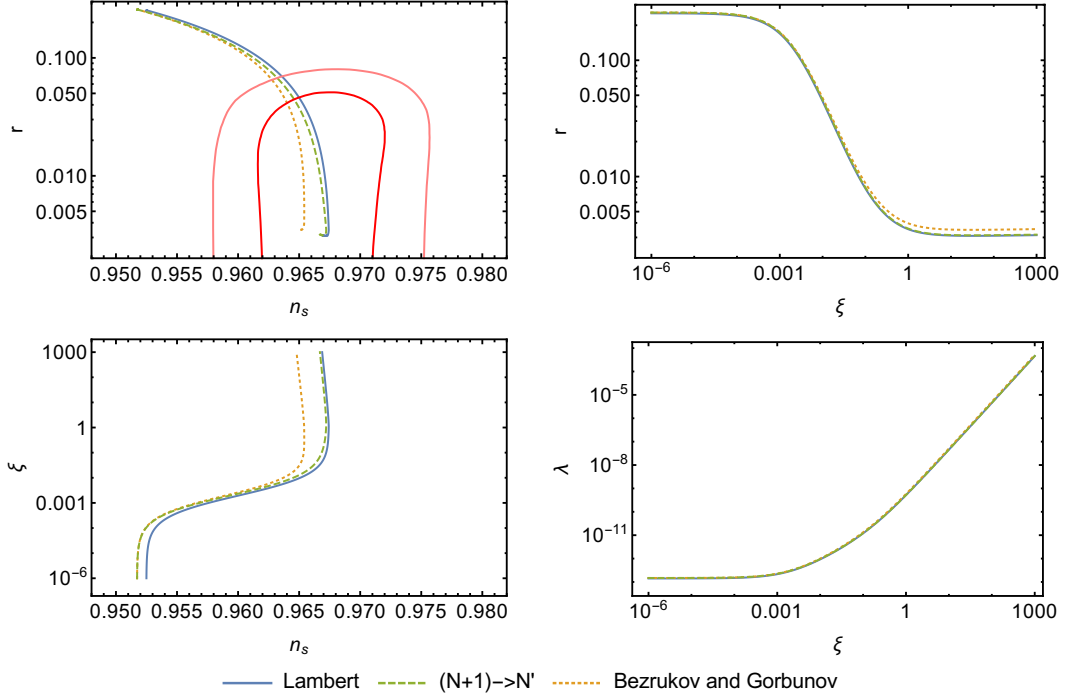


**Figure 1.** The values of  $n_s$ ,  $r$  and  $\lambda$  are shown as a function of the non-minimal coupling parameter  $\xi$ . “Lambert” curves show numerical solutions that are obtained using eq. (3.6), “Bezrukov and Gorbunov” curves show the approximate analytical expressions in ref. [43],  $(N + 1) \rightarrow N'$  curves show the improved analytical expressions using eq. (3.8). The pink (red) contour corresponds to the 95% (68%) CL constraint based on data taken by the Keck Array/BICEP2 and Planck collaborations [44].

a cut-off scale  $\Lambda = 1/\xi$  [48–50]. From eqs. (2.7) and (2.6), we obtain  $V = (3/2)\pi^2 r \Delta_{\mathcal{R}}^2$ . Thus, requiring  $\Lambda$  to be higher than the energy scale during inflation corresponds to

$$\xi < \left(\frac{3}{2}\pi^2 r \Delta_{\mathcal{R}}^2\right)^{-1/4}, \quad (3.11)$$

leading to  $\xi \lesssim 10^{2.5}$ . For this reason all numerical results in the following sections will be displayed for  $\xi$  values up to  $10^3$ . With this constraint, taking into account the quadratic phase after inflation makes only a  $\lesssim 1$  difference in the  $N_*$  value. Furthermore, preheating effects can make this difference even smaller. Thus, the uncertainty in the observational parameter values due to the reheating stage is rather small for non-minimal quartic inflation. For instance, in figure 1 which shows  $n_s$  and  $r$  values for  $\xi$  up to  $10^3$ , the effect of the quadratic phase amounts to the barely visible hook-like part at the bottom end of the  $n_s$ – $r$  curves. Therefore, we will use the  $\omega_r = 1/3$  approximation hereafter.

Finally, we note that since we compare the numerical  $n_s$  and  $r$  values with the recent Keck Array/BICEP2 and Planck data [44], our constraints on  $\xi$  are slightly more stringent compared to earlier works. Namely, non-minimal quartic inflation is compatible with the Keck Array/BICEP2 and Planck data for  $\xi \gtrsim 0.005$  (0.01) at 95% (68%) confidence level (CL).

## 4 Radiative corrections

Interactions of the inflaton with other fields, required for efficient reheating, lead to radiative corrections in the inflaton potential. These corrections can be expressed at leading order as follows [51]:

$$\Delta V(\phi) = \sum_i \frac{(-1)^F}{64\pi^2} M_i(\phi)^4 \ln \left( \frac{M_i(\phi)^2}{\mu^2} \right), \quad (4.1)$$

where  $F$  is  $+1$  ( $-1$ ) for bosons (fermions),  $\mu$  is a renormalization scale and  $M_i(\phi)$  denote field dependent masses.

First let us consider the potential terms for a minimally coupled inflaton field with a quartic potential, which couples to another scalar  $\chi$  and to a Dirac fermion  $\Psi$ :

$$V(\phi, \chi, \Psi) = \frac{\lambda}{4} \phi^4 + h\phi \bar{\Psi} \Psi + m_\Psi \bar{\Psi} \Psi + \frac{1}{2} g^2 \phi^2 \chi^2 + \frac{1}{2} m_\chi^2 \chi^2. \quad (4.2)$$

Under the assumptions

$$g^2 \phi^2 \gg m_\chi^2, \quad g^2 \gg \lambda, \quad h\phi \gg m_\Psi, \quad h^2 \gg \lambda, \quad (4.3)$$

the inflaton potential including the Coleman-Weinberg (CW) one-loop corrections given by eq. (4.1) take the form:

$$V(\phi) = \frac{\lambda}{4} \phi^4 \pm \kappa \phi^4 \ln \left( \frac{\phi}{\mu} \right), \quad (4.4)$$

where the  $+$  ( $-$ ) sign corresponds to the case of the inflaton dominantly coupling to bosons (fermions) and we have defined the radiative correction coupling parameter

$$\kappa \equiv \frac{1}{32\pi^2} \left| (g^4 - 4h^4) \right|. \quad (4.5)$$

Generalizing eq. (4.4) to the non-minimally coupled case is subject to ambiguity unless the ultraviolet completion of the low-energy effective field theory is specified, as discussed in refs. [21, 22, 27, 52]. In the literature, typically two prescriptions for the calculation of radiative corrections are adopted. In prescription I, the field dependent masses in the one-loop CW potential are expressed in the Einstein frame. Using the transformations

$$V(\phi) = \frac{V_J(\phi)}{F(\phi)^2}, \quad \tilde{\phi} = \frac{\phi}{\sqrt{F(\phi)}}, \quad \tilde{\Psi} = \frac{\Psi}{F(\phi)^{3/4}}, \quad \tilde{m}_\Psi(\phi) = \frac{m_\Psi(\phi)}{\sqrt{F(\phi)}}, \quad \tilde{m}_\chi^2 = \frac{m_\chi^2}{F(\phi)}, \quad (4.6)$$

the one-loop corrected potential is obtained in the Einstein frame as

$$V(\phi) = \frac{\frac{\lambda}{4} \phi^4 \pm \kappa \phi^4 \ln \left( \frac{\phi}{\mu \sqrt{1+\xi\phi^2}} \right)}{(1+\xi\phi^2)^2}. \quad (4.7)$$

In prescription II, the field dependent masses in the one-loop CW potential are expressed in the Jordan frame, so that eq. (4.4) corresponds to the one-loop corrected potential in the Jordan frame. Therefore the Einstein frame potential in this case is given by

$$V(\phi) = \frac{\frac{\lambda}{4} \phi^4 \pm \kappa \phi^4 \ln \left( \frac{\phi}{\mu} \right)}{(1+\xi\phi^2)^2}. \quad (4.8)$$

Note that the potentials in eqs. (4.7) and (4.8) are approximations that can be obtained from the one-loop renormalization group improved effective actions, see for instance ref. [28] for a discussion of this point.

In the next two sections, we numerically investigate how the  $n_s$  and  $r$  values change as a function of the coupling parameters  $\xi$  and  $\kappa$  using prescription I and prescription II, respectively. The calculation procedure is as follows: We form a grid of points in the  $\xi$  and  $\kappa$  plane. For each  $(\xi, \kappa)$  point, we start the calculation by assigning an initial  $\lambda$  value. We then calculate numerical values of  $\phi_e$  using  $\epsilon(\phi_e) = 1$ , and  $\phi_*$  using eq. (2.11). The e-fold number  $N_*$  is calculated using eq. (2.12) and compared with eq. (2.14). The initial value of  $\lambda$  is then adjusted and the calculation is repeated until the two  $N_*$  values match. The  $\phi_*$  value obtained this way is plugged in eqs. (2.9) and (2.6) to yield the  $n_s$  and  $r$  values. Finally, the calculation is repeated over the whole grid, with  $\lambda$  solutions for each point used as initial values of their neighbors.

For the numerical calculations, a value for  $\mu$  should also be specified. However, shifting the value of  $\mu$  does not change the forms of eqs. (4.7) and (4.8), corresponding only to a shift in the value of  $\lambda$ . Thus, for fixed values of the coupling parameters  $\xi$  and  $\kappa$ ,  $n_s$  and  $r$  values do not depend on  $\mu$ .

## 5 Radiatively corrected quartic potential: Prescription I

In this section we numerically investigate how the  $n_s$  and  $r$  values change as a function of the coupling parameters  $\xi$  and  $\kappa$ , using the potential in eq. (4.7), with a  $+$  ( $-$ ) sign for the inflaton dominantly coupling to bosons (fermions).

For prescription I and inflaton coupling to bosons, figure 2 shows the region in the  $\xi$  and  $\kappa$  plane where  $n_s$  and  $r$  values are compatible with the current data. Figure 3 shows how  $n_s$  and  $r$  values change with  $\kappa$  for chosen  $\xi$  values. It is clear from the figures that  $n_s$  and  $r$  values depend more sensitively on the value of  $\xi$  rather than  $\kappa$ . As  $\kappa$  is increased holding  $\xi$  fixed, there is a transition in  $n_s$  and  $r$  values for a relatively narrow range of  $\kappa$ .  $n_s$  and  $r$  no longer change at even larger  $\kappa$  values, however this last result is subject to some caveats as discussed below.

In contrast to the other cases covered in subsequent sections, we find that eqs. (2.11), (2.12) and (2.14) can be simultaneously satisfied for arbitrarily large values of  $\kappa$ . However, as mentioned in section 4, the potential we use is an approximation of the one-loop renormalization group improved effective action, and this approximation will eventually fail for large values of  $\kappa$ . Furthermore, higher loop corrections will eventually become also important.

Even if we take the potential in eq. (4.7) at face value, the inflationary solutions for large  $\kappa$  values can only be obtained for fine tuned values of the coupling parameters. To show this, let us write the potential in the limit  $\xi\phi^2 \gg 1$  and take  $\mu = 1$  for convenience. The potential then approximately takes the form eq. (3.1), with  $\lambda/4$  replaced by  $A \equiv \lambda/4 - (\kappa/2) \ln \xi$ . Using eq. (2.4), this potential can be written as

$$V(\sigma) \approx \frac{A}{\xi^2} \left[ 1 - 2 \exp \left( -2\sqrt{\frac{s}{6}}\sigma \right) \right]. \quad (5.1)$$

Using eq. (2.8),  $\exp(2\sqrt{s/6}\sigma) \approx 4sN/3$ . Finally, using eq. (2.7), we obtain

$$\lambda \approx \frac{72\pi^2 \Delta_R^2 \xi^2}{sN^2} + 2\kappa \ln \xi. \quad (5.2)$$

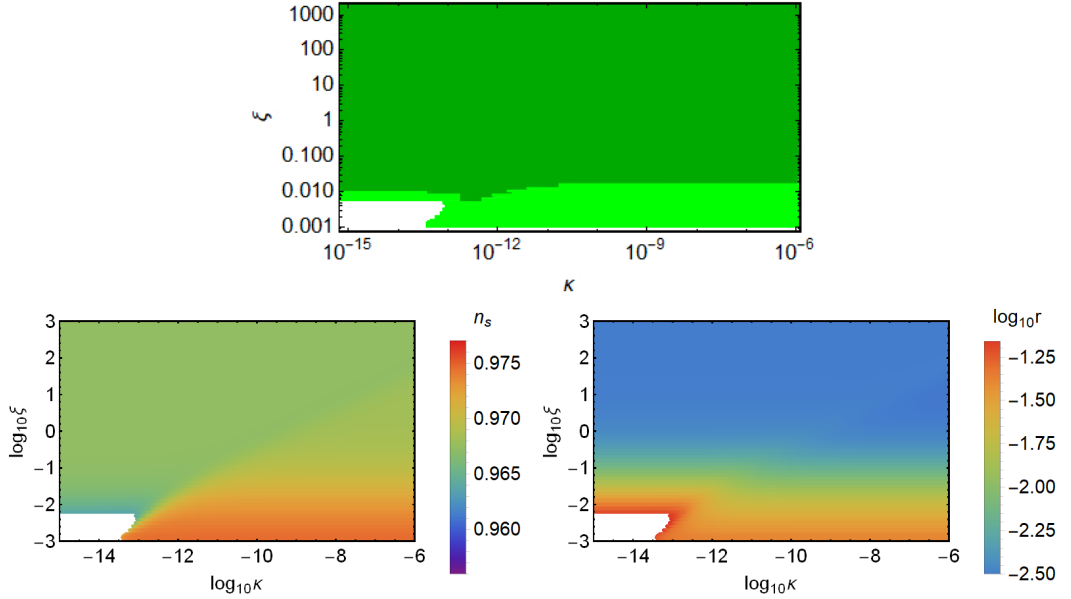


**Figure 2.** For prescription I and inflaton coupling to bosons, the top figure shows in light green (green) the regions in the  $\xi$ - $\kappa$  plane for which  $n_s$  and  $r$  values are within the 95% (68%) CL contours based on data taken by the Keck Array/BICEP2 and Planck collaborations [44]. Bottom figures show  $n_s$  and  $r$  values in these regions.

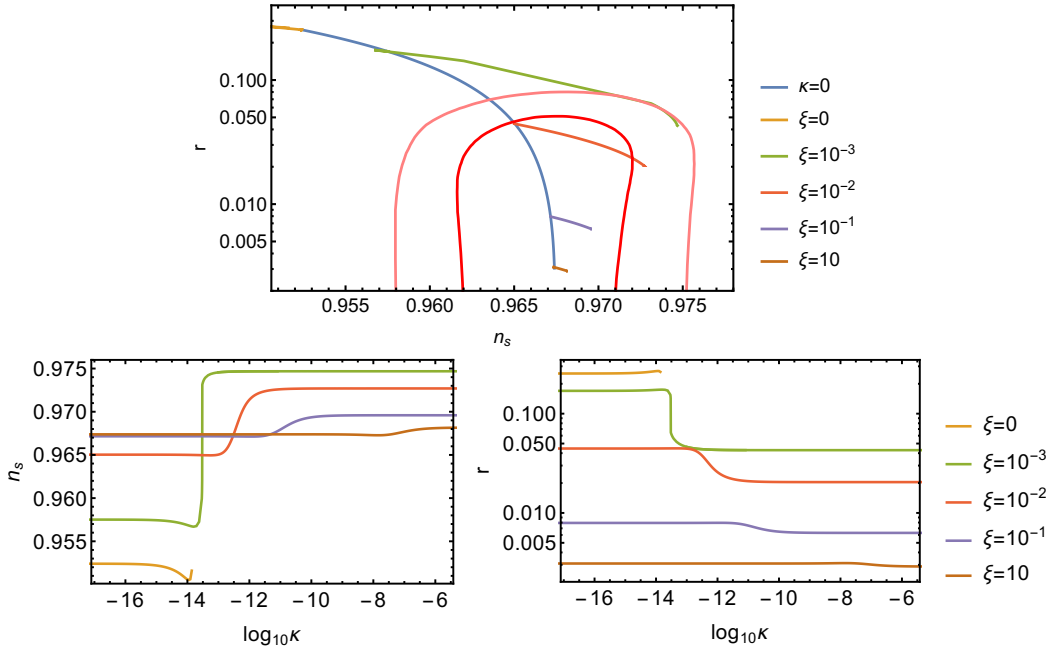


**Figure 3.** For prescription I and inflaton coupling to bosons, the change in  $n_s$  and  $r$  as a function of  $\kappa$  is plotted for selected  $\xi$  values. The pink (red) contour in the top figure corresponds to the 95% (68%) CL contour based on data taken by the Keck Array/BICEP2 and Planck collaborations [44].

The first term in the right hand side is approximately  $5 \times 10^{-10} \xi^2$  for  $\xi \gg 1$ . If  $2\kappa \ln \xi$  is much larger than this term, eq. (5.2) can only be satisfied if  $\lambda$  almost exactly equals  $2\kappa \ln \xi$ .

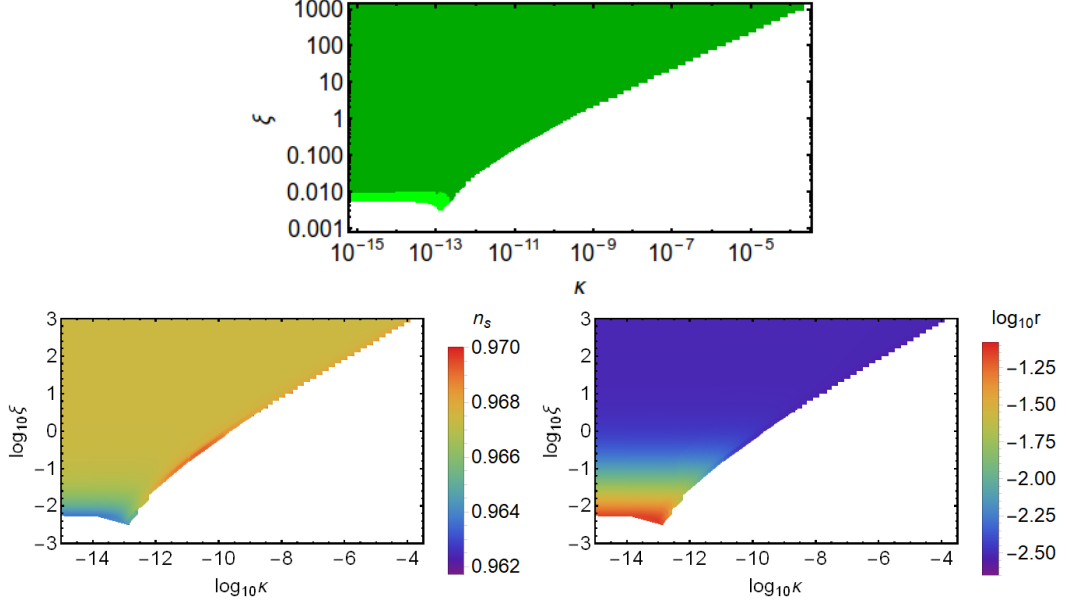


**Figure 4.** For prescription I, inflaton coupling to fermions and first branch solutions, the top figure shows in light green (green) the regions in the  $\xi$ – $\kappa$  plane for which  $n_s$  and  $r$  values are within the 95% (68%) CL contours based on data taken by the Keck Array/BICEP2 and Planck collaborations [44]. Bottom figures show  $n_s$  and  $r$  values in these regions.

The case of inflaton having a quartic potential with radiative corrections due to coupling to fermions was discussed in ref. [53] taking  $\xi = 0$ . There it was pointed out that there are two solutions for every  $\kappa$  value that is smaller than a maximum  $\kappa_{\max}$  value. This is also true for  $\xi \neq 0$ , with  $\kappa_{\max}$  values depending on  $\xi$ . We label the branch of solutions with larger  $\lambda$  for a given  $\kappa$  as the first branch, and the other branch of solutions as the second branch. For  $\kappa > \kappa_{\max}$  there is no solution, that is, eqs. (2.11), (2.12) and (2.14) cannot be simultaneously satisfied.

For prescription I and inflaton coupling to fermions, figure 4 shows the region in the  $\xi$  and  $\kappa$  plane where  $n_s$  and  $r$  values are compatible with the current data, for the first branch of solutions. Again,  $n_s$  and  $r$  values depend more sensitively on the value of  $\xi$  rather than  $\kappa$ . The observationally compatible region for the second branch of solutions is shown in figure 5. As seen from the figure, the second branch solutions are compatible with observations for only a narrow region in the  $\xi$ – $\kappa$  plane.

Figure 6 shows how  $n_s$  and  $r$  values change with  $\kappa$  and the  $\kappa_{\max}$  values for chosen  $\xi$  values. The first branch solutions move from the red points towards the  $\kappa = 0$  curve as  $\kappa$  decreases. As can be seen from the bottom panels, significant change in the  $n_s$  and  $r$  values only occur when  $\kappa$  becomes the same order of magnitude as  $\kappa_{\max}$ . The second branch solutions, on the other hand, move towards small  $n_s$  values and away from the observationally favored region in the  $n_s$ – $r$  plane as  $\kappa$  decreases. These solutions cease to exist for  $\kappa \ll \kappa_{\max}$  as inflation with sufficient duration cannot be obtained.

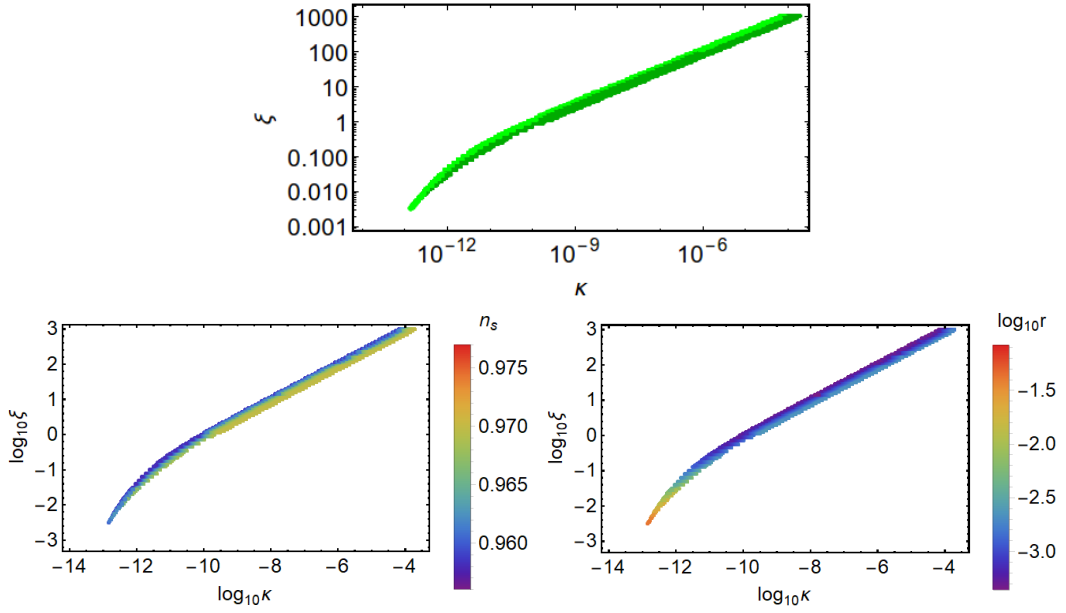


**Figure 5.** For prescription I, inflaton coupling to fermions and second branch solutions, the top figure shows in light green (green) the regions in the  $\xi$ - $\kappa$  plane for which  $n_s$  and  $r$  values are within the 95% (68%) CL contours based on data taken by the Keck Array/BICEP2 and Planck collaborations [44]. Bottom figures show  $n_s$  and  $r$  values in these regions.

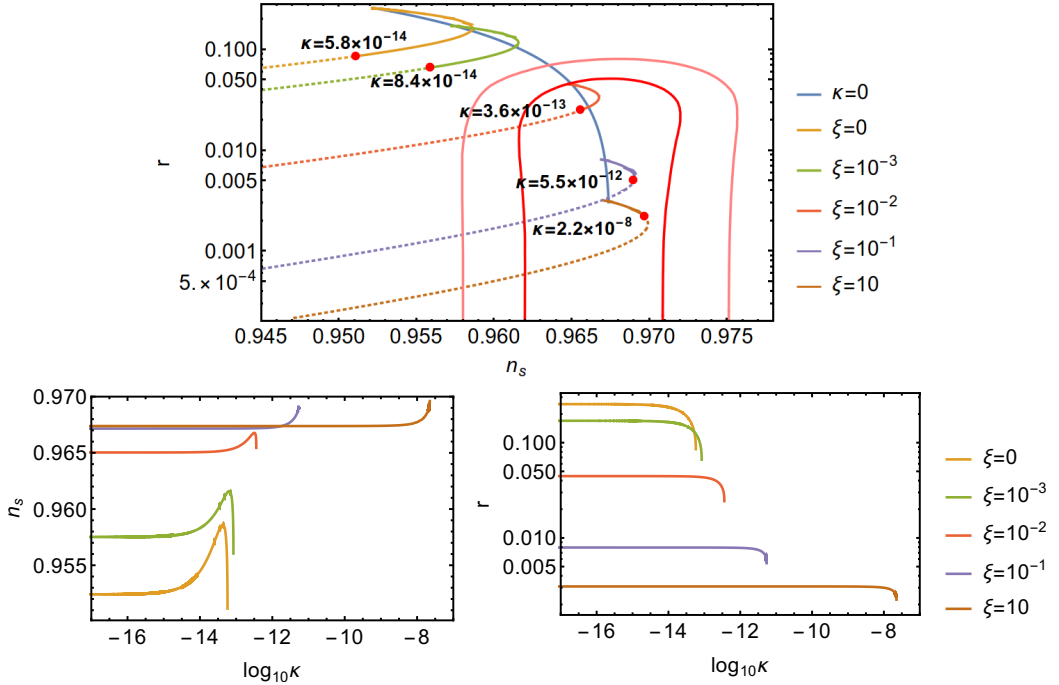


**Figure 6.** For prescription I and inflaton coupling to fermions, the change in  $n_s$  and  $r$  as a function of  $\kappa$  is plotted for selected  $\xi$  values. The pink (red) contour in the top figure corresponds to the 95% (68%) CL contour based on data taken by the Keck Array/BICEP2 and Planck collaborations [44]. The solid (dotted) portions of the curves correspond to first (second) branch of solutions. The red points show the maximum  $\kappa$  values where the two branch of solutions meet. These values are also written in the figure. The bottom figures only show the first branch solutions.

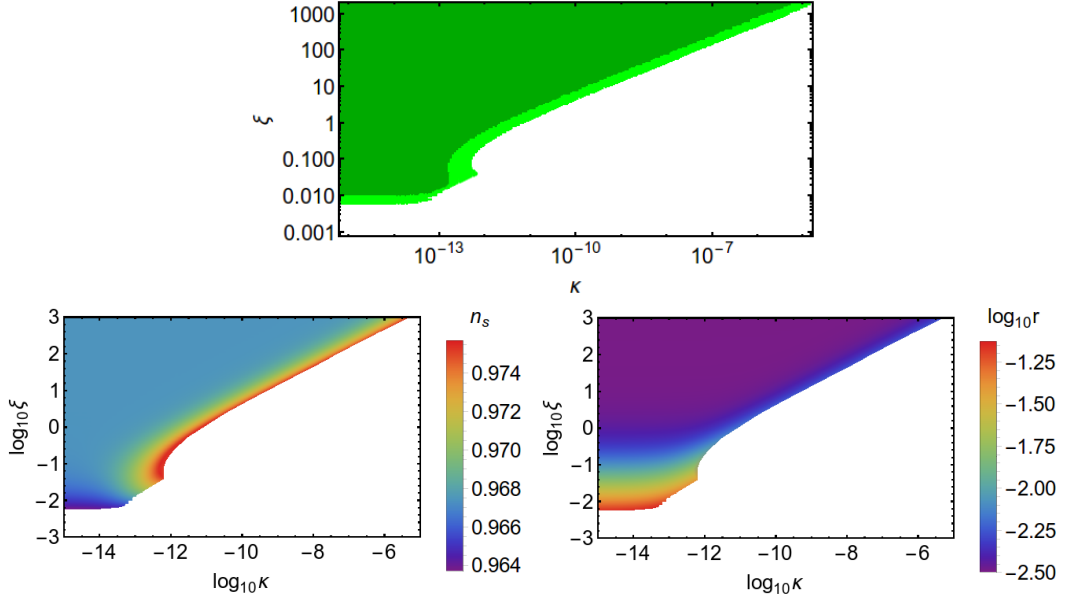


**Figure 7.** For prescription II and inflaton coupling to bosons, the top figure shows in light green (green) the regions in the  $\xi$ – $\kappa$  plane for which  $n_s$  and  $r$  values are within the 95% (68%) CL contours based on data taken by the Keck Array/BICEP2 and Planck collaborations [44]. Bottom figures show  $n_s$  and  $r$  values in these regions.

## 6 Radiatively corrected quartic potential: Prescription II

In this section we numerically investigate how the  $n_s$  and  $r$  values change as a function of the coupling parameters  $\xi$  and  $\kappa$ , using the potential in eq. (4.8), with a  $+$  ( $-$ ) sign for the inflaton dominantly coupling to bosons (fermions).

For prescription II and inflaton coupling to bosons, figure 7 shows the region in the  $\xi$  and  $\kappa$  plane where  $n_s$  and  $r$  values are compatible with the current data. Figure 8 shows how  $n_s$  and  $r$  values change with  $\kappa$  for chosen  $\xi$  values. The  $\kappa_{\max}$  values, that is, the maximum  $\kappa$  values that allow a simultaneous solution of eqs. (2.11), (2.12) and (2.14) are also shown. From the figures we see that for  $\xi \gtrsim 10^{-2}$ , the  $n_s$  and  $r$  values approach the linear potential predictions  $n_s \approx 1 - 3/(2N)$  ve  $r \approx 4/N$  as  $\kappa$  approaches  $\kappa_{\max}$ . This result is not surprising since for large enough  $\xi$  values  $\xi\phi^2 \gg 1$  during inflation, in which case the Einstein frame potential written in terms of the canonical scalar field using eqs. (2.3) and (2.4) contains a linear term which eventually dominates as the value of  $\kappa$  is increased. This approach to the linear potential predictions was also noted in refs. [7, 32, 33]. Similarly to the prescription I case for inflaton coupling to fermions, significant change in the  $n_s$  and  $r$  values only occur when  $\kappa$  becomes the same order of magnitude as  $\kappa_{\max}$ .

Similarly to the prescription I case, there are also two branch of solutions for prescription II and inflaton coupling to fermions. Figure 9 shows the region in the  $\xi$  and  $\kappa$  plane where  $n_s$  and  $r$  values are compatible with the current data, for the first branch of solutions. The second branch of solutions are not compatible with the current data at any value of  $\xi$  or  $\kappa$ . Figure 10 shows how  $n_s$  and  $r$  values change with  $\kappa$  and the  $\kappa_{\max}$  values for chosen  $\xi$  values. Again, the first branch solutions move from the red points towards the  $\kappa = 0$  curve as  $\kappa$  decreases, whereas the second branch solutions move towards small  $n_s$  values.

Finally we note that our results for prescription II and inflaton coupling to fermions overlap and agree with those of ref. [28].

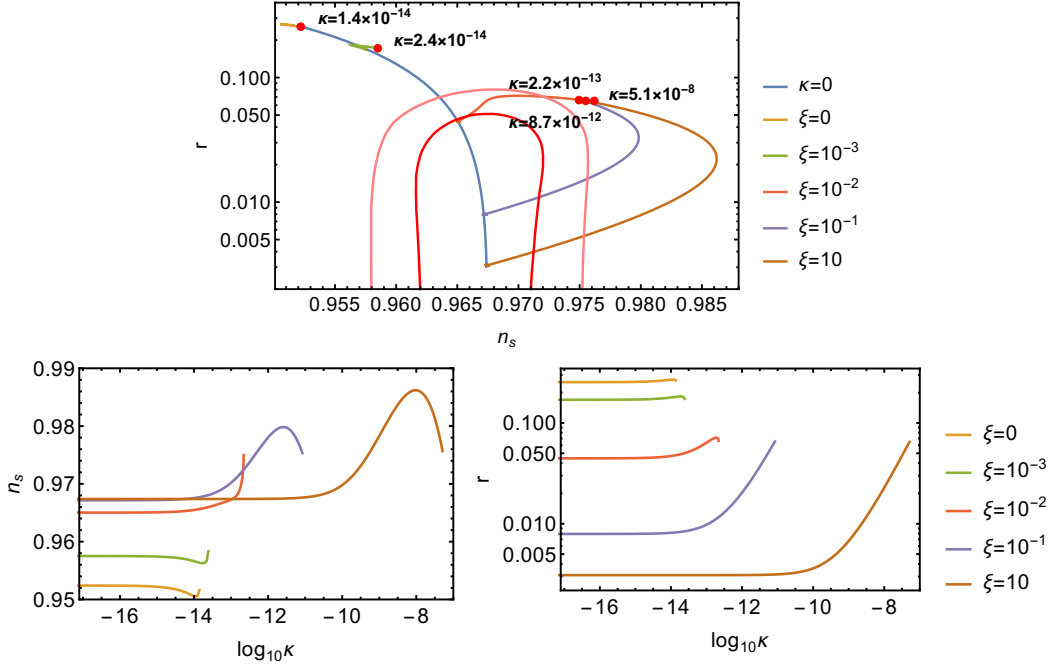


**Figure 8.** For prescription II and inflaton coupling to bosons, the change in  $n_s$  and  $r$  as a function of  $\kappa$  is plotted for selected  $\xi$  values. The pink (red) contour in the top figure corresponds to the 95% (68%) CL contour based on data taken by the Keck Array/BICEP2 and Planck collaborations [44]. The red points show the maximum  $\kappa$  values. These values, increasing with  $\xi$ , are also written in the figure.

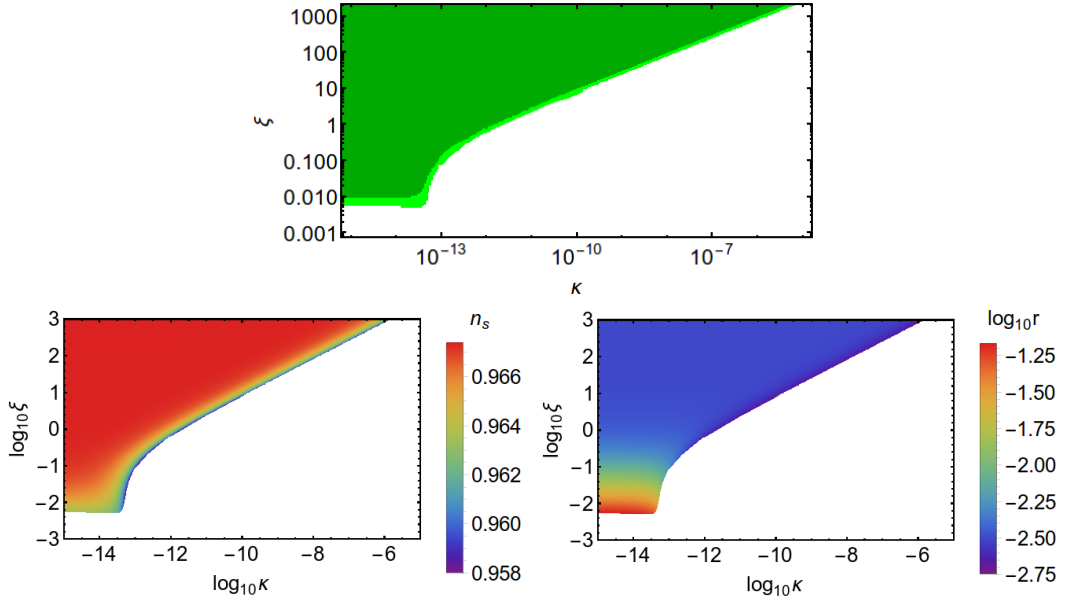


**Figure 9.** For prescription II, inflaton coupling to fermions and first branch solutions, the top figure shows in light green (green) the regions in the  $\xi-\kappa$  plane for which  $n_s$  and  $r$  values are within the 95% (68%) CL contours based on data taken by the Keck Array/BICEP2 and Planck collaborations [44]. Bottom figures show  $n_s$  and  $r$  values in these regions.

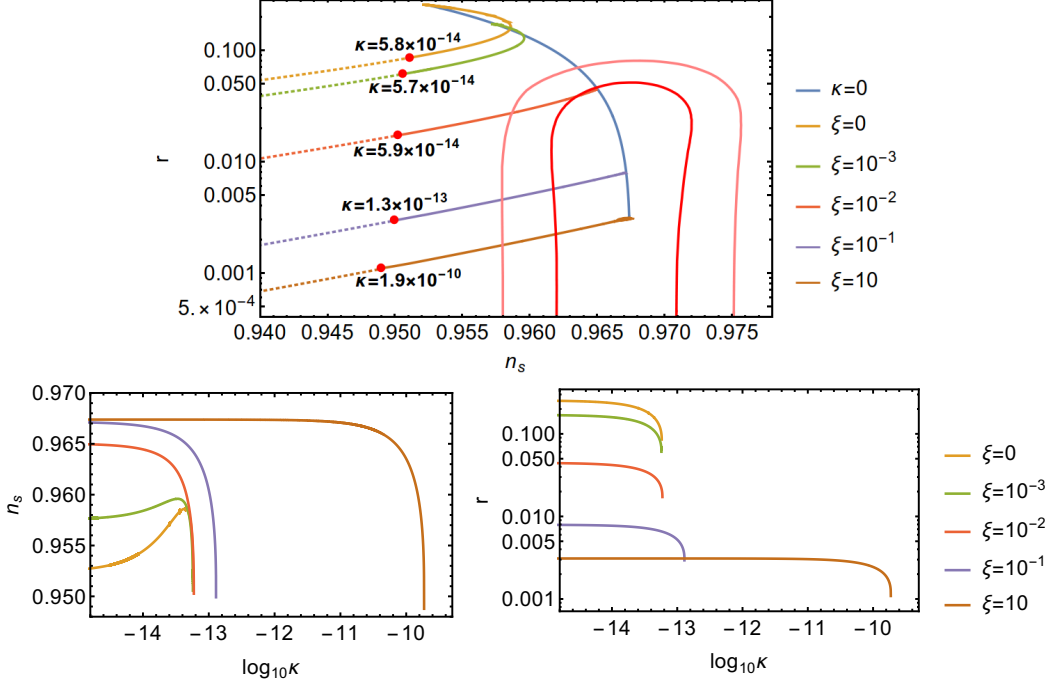


**Figure 10.** For prescription II and inflaton coupling to fermions, the change in  $n_s$  and  $r$  as a function of  $\kappa$  is plotted for selected  $\xi$  values. The pink (red) contour in the top figure corresponds to the 95% (68%) CL contour based on data taken by the Keck Array/BICEP2 and Planck collaborations [44]. The solid (dotted) portions of the curves correspond to first (second) branch of solutions. The red points show the maximum  $\kappa$  values where the two branch of solutions meet. These values are also written in the figure. The bottom figures only show the first branch solutions.

## 7 Conclusion

In this paper we revisited the non-minimal quartic inflation model consisting of a quartic potential and a coupling term  $\xi \phi^2 R$  between the Ricci scalar and the inflaton, first reviewing the tree level case without any radiative corrections in section 3. We noted that the approximate analytical expressions in ref. [43] can be improved by using the  $W_{-1}(-x) \approx \ln x - \ln(-\ln x)$  approximation for the Lambert function.

Two prescriptions used in the literature to take into account the radiative corrections to the potential were briefly discussed in section 4. We then numerically investigated the effect of the radiative corrections on the inflationary observables  $n_s$  and  $r$  due to inflaton coupling to bosons or fermions in section 5 for prescription I and in section 6 for prescription II.

Generally, we observed that while the radiative corrections prevent inflation with a sufficient duration after a  $\xi$  dependent maximum value  $\kappa_{\max}$  of the coupling parameter  $\kappa$  defined by eq. (4.5), they don't change  $n_s$  and  $r$  values significantly unless  $\kappa$  is the same order of magnitude as  $\kappa_{\max}$ . For the prescription I and coupling to bosons case, in contrast to the other cases, we found that eqs. (2.11), (2.12) and (2.14) can be simultaneously satisfied for arbitrarily large values of  $\kappa$ . However, as explained in section 5, we regard this result as an artifact of the approximation we used for the potential.

The two prescriptions for the radiative corrections lead to significantly different potentials in the limit  $\xi \phi^2 \gg 1$ , corresponding to  $\xi \gg 1/(8N)$ . For prescription I, the plateau type structure of the potential remains intact in this limit. As a result, for the same  $\kappa$  value the

effect of radiative corrections is milder compared to the results obtained using prescription II. This difference is also reflected in the  $\kappa_{\max}$  values. For example, if inflaton couples to fermions and  $\xi = 10$ ,  $\kappa_{\max}$  is  $2.2 \times 10^{-8}$  ( $1.9 \times 10^{-10}$ ) using prescription I (prescription II). Such differences suggest the need for further work on the theoretical motivations of these prescriptions used in the literature to calculate the observational parameters.

## Acknowledgements

This work is supported by TÜBİTAK (The Scientific and Technological Research Council of Turkey) project number 116F385.

## References

- [1] A. H. Guth, *The inflationary universe: A possible solution to the horizon and flatness problems*, *Phys. Rev.* **D23** (1981) 347.
- [2] A. D. Linde, *A new inflationary universe scenario: A possible solution of the horizon, flatness, homogeneity, isotropy and primordial monopole problems*, *Phys. Lett.* **108B** (1982) 389.
- [3] A. Albrecht and P. J. Steinhardt, *Cosmology for grand unified theories with radiatively induced symmetry breaking*, *Phys. Rev. Lett.* **48** (1982) 1220.
- [4] A. D. Linde, *Chaotic inflation*, *Phys. Lett.* **129B** (1983) 177.
- [5] PLANCK collaboration, N. Aghanim et al., *Planck 2018 results. VI. Cosmological parameters*, [1807.06209](#).
- [6] PLANCK collaboration, Y. Akrami et al., *Planck 2018 results. X. Constraints on inflation*, [1807.06211](#).
- [7] J. Martin, C. Ringeval and V. Vennin, *Encyclopædia inflationaris*, *Phys. Dark Univ.* **5-6** (2014) 75 [[1303.3787](#)].
- [8] C. G. Callan, Jr., S. R. Coleman and R. Jackiw, *A new improved energy - momentum tensor*, *Annals Phys.* **59** (1970) 42.
- [9] D. Z. Freedman and E. J. Weinberg, *The energy-momentum tensor in scalar and gauge field theories*, *Annals Phys.* **87** (1974) 354.
- [10] I. L. Buchbinder, S. D. Odintsov and I. L. Shapiro, *Effective action in quantum gravity*. IOP Publishing Ltd, 1992.
- [11] L. F. Abbott, *Gravitational effects on the SU(5) breaking phase transition for a Coleman-Weinberg potential*, *Nucl. Phys.* **B185** (1981) 233.
- [12] B. L. Spokoiny, *Inflation and generation of perturbations in broken symmetric theory of gravity*, *Phys. Lett.* **147B** (1984) 39.
- [13] F. Lucchin, S. Matarrese and M. D. Pollock, *Inflation with a nonminimally coupled scalar field*, *Phys. Lett.* **167B** (1986) 163.
- [14] T. Futamase and K.-i. Maeda, *Chaotic inflationary scenario in models having nonminimal coupling with curvature*, *Phys. Rev.* **D39** (1989) 399.
- [15] R. Fakir and W. G. Unruh, *Improvement on cosmological chaotic inflation through nonminimal coupling*, *Phys. Rev.* **D41** (1990) 1783.
- [16] D. S. Salopek, J. R. Bond and J. M. Bardeen, *Designing density fluctuation spectra in inflation*, *Phys. Rev.* **D40** (1989) 1753.

[17] L. Amendola, M. Litterio and F. Occhionero, *The phase space view of inflation. 1: The nonminimally coupled scalar field*, *Int. J. Mod. Phys. A* **5** (1990) 3861.

[18] V. Faraoni, *Nonminimal coupling of the scalar field and inflation*, *Phys. Rev. D* **53** (1996) 6813 [[astro-ph/9602111](#)].

[19] V. Faraoni, *Cosmology in scalar tensor gravity*. Kluwer Academic Publishers, 2004.

[20] F. L. Bezrukov and M. Shaposhnikov, *The standard model Higgs boson as the inflaton*, *Phys. Lett. B* **659** (2008) 703 [[0710.3755](#)].

[21] F. Bezrukov, *The Higgs field as an inflaton*, *Class. Quant. Grav.* **30** (2013) 214001 [[1307.0708](#)].

[22] F. Bezrukov and M. Shaposhnikov, *Standard model Higgs boson mass from inflation: Two loop analysis*, *JHEP* **07** (2009) 089 [[0904.1537](#)].

[23] E. Komatsu and T. Futamase, *Complete constraints on a nonminimally coupled chaotic inflationary scenario from the cosmic microwave background*, *Phys. Rev. D* **59** (1999) 064029 [[astro-ph/9901127](#)].

[24] S. Tsujikawa and B. Gumjudpai, *Density perturbations in generalized Einstein scenarios and constraints on nonminimal couplings from the cosmic microwave background*, *Phys. Rev. D* **69** (2004) 123523 [[astro-ph/0402185](#)].

[25] A. A. Starobinsky, *A new type of isotropic cosmological models without singularity*, *Phys. Lett. B* **91** (1980) 99.

[26] A. Kehagias, A. Moradinezhad Dizgah and A. Riotto, *Remarks on the Starobinsky model of inflation and its descendants*, *Phys. Rev. D* **89** (2014) 043527 [[1312.1155](#)].

[27] F. L. Bezrukov, A. Magnin and M. Shaposhnikov, *Standard model Higgs boson mass from inflation*, *Phys. Lett. B* **675** (2009) 88 [[0812.4950](#)].

[28] N. Okada, M. U. Rehman and Q. Shafi, *Tensor to scalar ratio in non-minimal  $\phi^4$  inflation*, *Phys. Rev. D* **82** (2010) 043502 [[1005.5161](#)].

[29] R. N. Lerner and J. McDonald, *Gauge singlet scalar as inflaton and thermal relic dark matter*, *Phys. Rev. D* **80** (2009) 123507 [[0909.0520](#)].

[30] R. N. Lerner and J. McDonald, *Distinguishing Higgs inflation and its variants*, *Phys. Rev. D* **83** (2011) 123522 [[1104.2468](#)].

[31] F. Kahlhoefer and J. McDonald, *WIMP dark matter and unitarity-conserving inflation via a gauge singlet scalar*, *JCAP* **1511** (2015) 015 [[1507.03600](#)].

[32] A. Racioppi, *New universal attractor in nonminimally coupled gravity: Linear inflation*, *Phys. Rev. D* **97** (2018) 123514 [[1801.08810](#)].

[33] M. Rinaldi, L. Vanzo, S. Zerbini and G. Venturi, *Inflationary quasiscale-invariant attractors*, *Phys. Rev. D* **93** (2016) 024040 [[1505.03386](#)].

[34] N. Okada and D. Raut, *Running non-minimal inflation with stabilized inflaton potential*, *Eur. Phys. J. C* **77** (2017) 247 [[1509.04439](#)].

[35] L. Marzola, A. Racioppi, M. Raidal, F. R. Urban and H. Veermäe, *Non-minimal CW inflation, electroweak symmetry breaking and the 750 GeV anomaly*, *JHEP* **03** (2016) 190 [[1512.09136](#)].

[36] L. Marzola and A. Racioppi, *Minimal but non-minimal inflation and electroweak symmetry breaking*, *JCAP* **1610** (2016) 010 [[1606.06887](#)].

[37] Y. Fujii and K. Maeda, *The scalar-tensor theory of gravitation*. Cambridge University Press, 2007.

[38] D. H. Lyth and A. R. Liddle, *The primordial density perturbation: Cosmology, inflation and the origin of structure*. Cambridge University Press, 2009.

[39] A. Linde, M. Noorbala and A. Westphal, *Observational consequences of chaotic inflation with nonminimal coupling to gravity*, *JCAP* **1103** (2011) 013 [[1101.2652](#)].

[40] A. R. Liddle and S. M. Leach, *How long before the end of inflation were observable perturbations produced?*, *Phys. Rev.* **D68** (2003) 103503 [[astro-ph/0305263](#)].

[41] D. I. Kaiser, *Primordial spectral indices from generalized Einstein theories*, *Phys. Rev.* **D52** (1995) 4295 [[astro-ph/9408044](#)].

[42] F. L. Bezrukov, *Non-minimal coupling in inflation and inflating with the Higgs boson*, [0810.3165](#).

[43] F. Bezrukov and D. Gorbunov, *Light inflaton after LHC8 and WMAP9 results*, *JHEP* **07** (2013) 140 [[1303.4395](#)].

[44] BICEP2, KECK ARRAY collaboration, P. A. R. Ade et al., *BICEP2 / Keck Array x: Constraints on primordial gravitational waves using Planck, WMAP, and new BICEP2/Keck observations through the 2015 season*, *Phys. Rev. Lett.* **121** (2018) 221301 [[1810.05216](#)].

[45] M. S. Turner, *Coherent scalar field oscillations in an expanding universe*, *Phys. Rev.* **D28** (1983) 1243.

[46] F. Bezrukov, D. Gorbunov and M. Shaposhnikov, *On initial conditions for the hot big bang*, *JCAP* **0906** (2009) 029 [[0812.3622](#)].

[47] J.-O. Gong, S. Pi and G. Leung, *Probing reheating with primordial spectrum*, *JCAP* **1505** (2015) 027 [[1501.03604](#)].

[48] C. P. Burgess, H. M. Lee and M. Trott, *Power-counting and the validity of the classical approximation during inflation*, *JHEP* **09** (2009) 103 [[0902.4465](#)].

[49] J. L. F. Barbon and J. R. Espinosa, *On the naturalness of Higgs inflation*, *Phys. Rev.* **D79** (2009) 081302 [[0903.0355](#)].

[50] M. P. Hertzberg, *On inflation with non-minimal coupling*, *JHEP* **11** (2010) 023 [[1002.2995](#)].

[51] S. R. Coleman and E. J. Weinberg, *Radiative corrections as the origin of spontaneous symmetry breaking*, *Phys. Rev.* **D7** (1973) 1888.

[52] Y. Hamada, H. Kawai, Y. Nakanishi and K.-y. Oda, *Meaning of the field dependence of the renormalization scale in Higgs inflation*, *Phys. Rev.* **D95** (2017) 103524 [[1610.05885](#)].

[53] V. N. Şenoğuz and Q. Shafi, *Chaotic inflation, radiative corrections and precision cosmology*, *Phys. Lett.* **B668** (2008) 6 [[0806.2798](#)].